

Laser Thermal Input Effects on Deep Penetration CO₂ Laser Welding of Carbon Steel

Saad A. Mohammed Salih
Department of Laser and
Optoelectronics Engineering
College of Engineering –Nahrain
University - Iraq

Walid K. Hamoudi
School of Applied Sciences –
University of Technology – Iraq

Adel K. Hamoudi
Department of Physics/College of
Science – University of Baghdad
– Iraq

Abstract

The present work brings forward a computational modeling of welding phenomena within an analytical framework. The aim is to study the effect of laser power and travel speed on the heat flow in keyhole laser welding and compare the experimental investigations with the theoretical model which was published formerly (ref.21,22). The problem is formulated and solved by approximating the laser beam as a point and a line heat source operating simultaneously. This concept produces weld profiles that have good qualitative agreement with the experiments. Mathematical model and computer program were constructed to solve two basic heat conduction equations for the moving point and line sources. The effect of coupling efficiency, thermal input and laser power loss on the welds parameters is presented.

Key words: laser welding, thermal input, coupling efficiency, penetration depth

1. Introduction

The intent in laser welding is to produce the liquid melt pool by absorption of incident radiation, allowing it to grow to the desired size, and then to propagate this melt pool through the solid interface eliminating the original seam between the components to be joined [1, 2, 3]. Constant heat dissipation within the work piece in the presence of a weld pool requires a stable geometry between the fusion front and the surrounding metal [4]. In keyhole welding, the laser beam allows delivering a large amount of energy to the point where it is needed the most. In addition laser welding can be performed at a relatively high speed [5, 6] but higher laser intensities are required. The choice of weld speed, keyhole size, laser power absorbed by the material, and the weld width depend on the material's temperature, thermal diffusivity, heat capacity, and thermal conductivity. Unsuccessful results are obtained if the melt pool is too large or too small or if significant vaporization occurs. Excessive thermal gradients lead to cracking on

solidification and instabilities in the volume and geometry of the weld pool that can result in porosity and void formation [7, 8]. Laser welded depth for a given material is determined mainly by the laser power, the focused spot diameter, and the processing speed, [9, 10, 11]. Once a keyhole is formed, then the welding speed affects the depth of penetration, weld width and the presence of dropout defects. Faster welds do not, in effect, have time to pass on much heat from the keyhole before it has moved on. Therefore, there is an optimum laser power and speed combination for the most effective penetration and largest weld depth to width ratio (aspect ratio). In CO₂ laser butt welding of AISI304, the effects of laser power, welding speed and focal point position on tensile strength, impact strength and joint-operating cost were investigated [12]. Mathematical models based on analysis of variance were formulated to identify the optimal welding conditions in order to increase the productivity and minimize the operating cost. In a 15 kW CO₂ laser welding of 12 mm thick steel, the stability of the keyhole can affect the properties of welded components and the plasma fluctuations [13]. It was found that the penetration depth increases sharply with increasing laser power but this power has a less influence on weld profile and HAZ width [14]. When a 10 kW fiber laser used to weld 304-austenitic stainless steel, an 18 mm penetration depth was reached at 5 mm/s in a nitrogen shield gas [15]. At higher or lower speeds; porosity, under-filling and humping weld beads were formed. The effects of laser power, welding travel speed and defocusing distance on the weld dimensions and the microstructure during CO₂ laser butt welding of Low carbon steel ST14 were investigated [16]. Variation in the metallographic morphologies of the weld has resulted, even with full penetration welds, due to very rapid solidification. In laser keyhole welding of Ti-6Al-4V, a 3-D model consisting of a rotary Gaussian volumetric heat source and a double ellipsoid heat source was developed to work out a simple solution and first order upwind discretization under-relaxation iteration [17]. The local

temperature distribution in the fusion zone was simulated separately with regard to dependence on laser power inputs and welding speeds. The results indicated that eddies occur near the top and bottom surfaces helped heat transfer and bulbous weld pool formation. Weld microstructure, heat affected zone widths, joint properties and distortion may play a role in weld cracking. These parameters are influenced by thermal input [18] which can be specified by the weld area as a measure of the heat absorbed [19, 20]. In previous publications [21, 22], we presented a mathematical 3-D model and a computer code for keyhole CO₂ laser welding of thick C/Mn steel sheets under variety of laser material processing conditions to study the weld profile, the temperature distribution and the heat affected zone. The model combined a moving point source for the top part of the weld and a moving line source for the parallel sided region of the weld (stem).

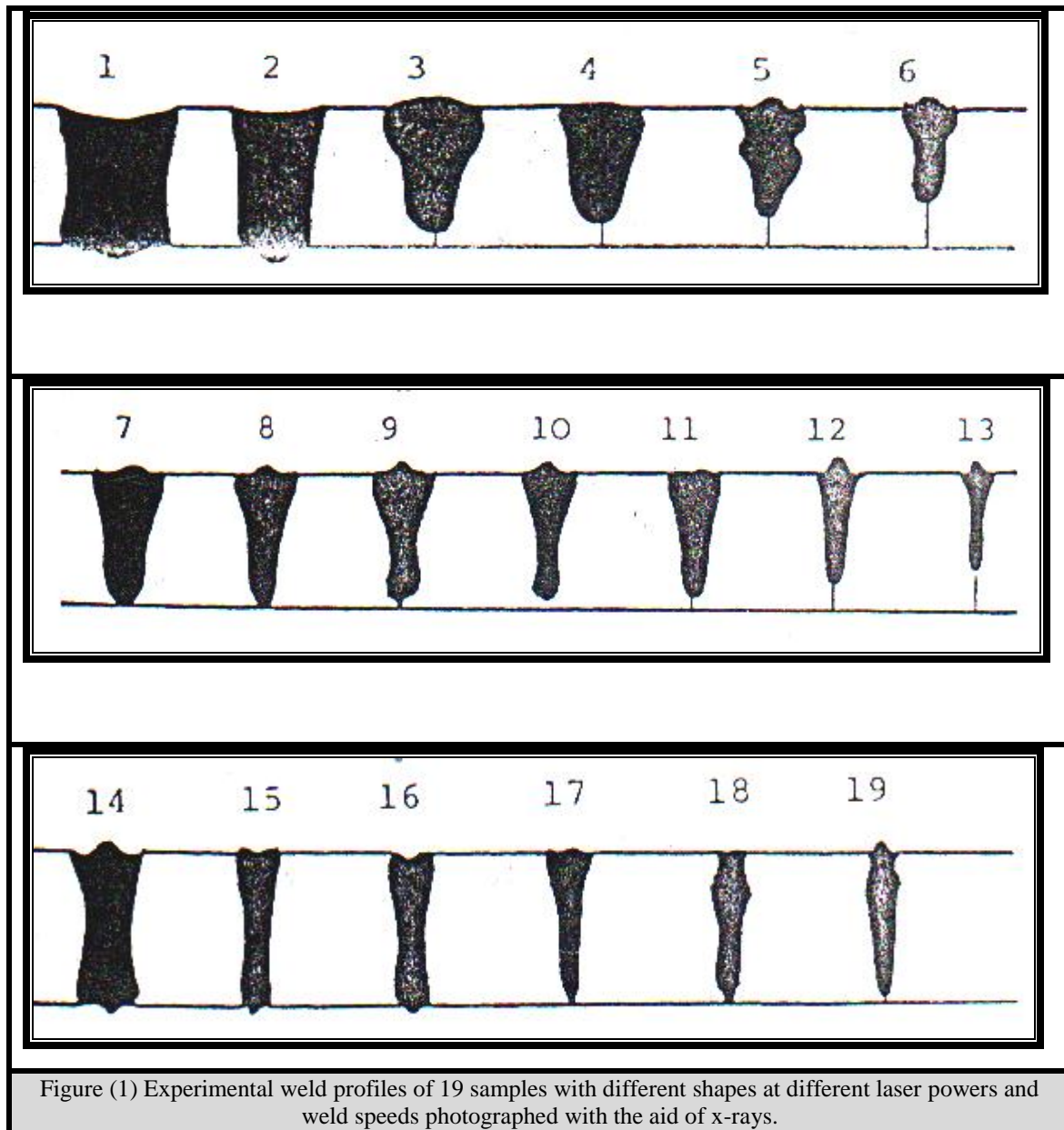
Welding velocity was measured by utilizing the sensors connected to the moving workpiece, thus, to the computer with high accuracy. This is all done in Cambridge welding institute.

In this study we present the effect of thermal input on the welds characteristics of carbon steel using a high power CO₂ laser. Experimental results are compared to those obtained from the computer simulation. Thermal input was found to be inversely proportional to coupling efficiency and Narrow weld profiles were obtained when using small thermal input values. Our simulation code may be used to automate laser welding process in the current sophisticated systems for 1, 2 and 3-D modeling and monitor robotic welding machines.

2. Experimental

A high power continuous wave CO₂ laser beam with pre-selected power values was used to perform butt-welding of 12 mm thick (BS4360) C/Mn steel. The effects of laser power and welding speed on welded depth, welded width and welded area were investigated. The laser source was operating in the TEM₀₁ mode so that a maximum output power could be achieved. The experimental parameters and physical constants of the laser beam and relevant material adopted in this work are shown in table-1. Figure (1) shows the 19 welds obtained from the experiment.

Table1: Laser data and Material parameters.		
	Laser and material parameters	Description
	Laser	CO₂
	Power (kW)	7.0, 8.5, 10
	Mode	TEM₀₁
	Focal spot (mm)	0.5
	Shielding gas jet	He, flow : 50 l/min
	Steel type	BS43660 C/Mn Steel.
	Thickness (mm)	12.0
	Thermal conductivity k (W/mm °C)	0.019385
	Thermal diffusivity K (mm²/s)	12.5
	Melting point (°C)	1547
	Ambient Temp. (°C)	27



3. Results and discussion

The weld profiles, obtained experimentally, were investigated numerically with specific choices of strengths of the point and line sources (λ and μ) and specific locations of the point source (c). The values of (λ and μ) were calculated and found to be [21]:

$$\frac{q_p U}{8\pi k K (T_m - T_0)} = \lambda,$$

and

$$\mu = \frac{q_l}{2\pi k (T_m - T_0)}$$

Where, q_p is the power absorbed by the point source in Watts, q_l is the power absorbed by the line source per unit length in Watts/mm, T_0 is the ambient temperature, T_m is the melting temperature, k is the thermal conductivity, and K is the thermal diffusivity. Figures (2 & 3) show the thermal input

is inversely proportional to the coupling efficiency in contrast to the behavior of the power or speed versus the same coupling efficiency. This shows the importance of the adjusting principle between power and speed in order to obtain good weld quality

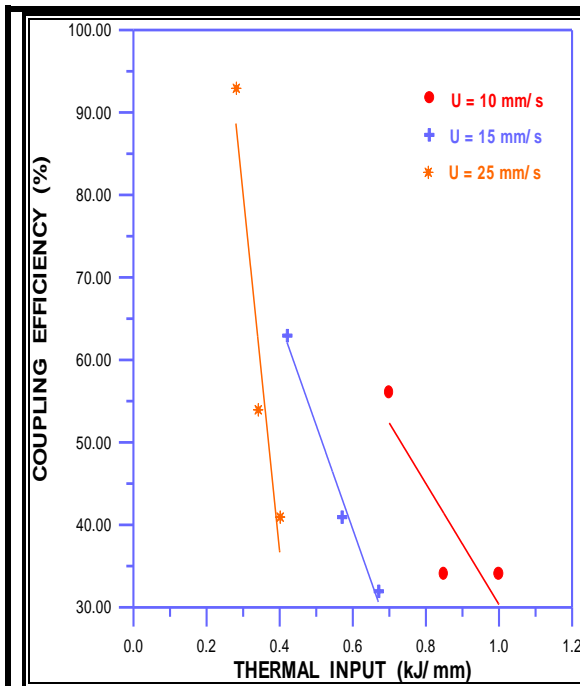


Figure (2): Thermal input versus coupling efficiency at a variable speeds and fixed laser power.

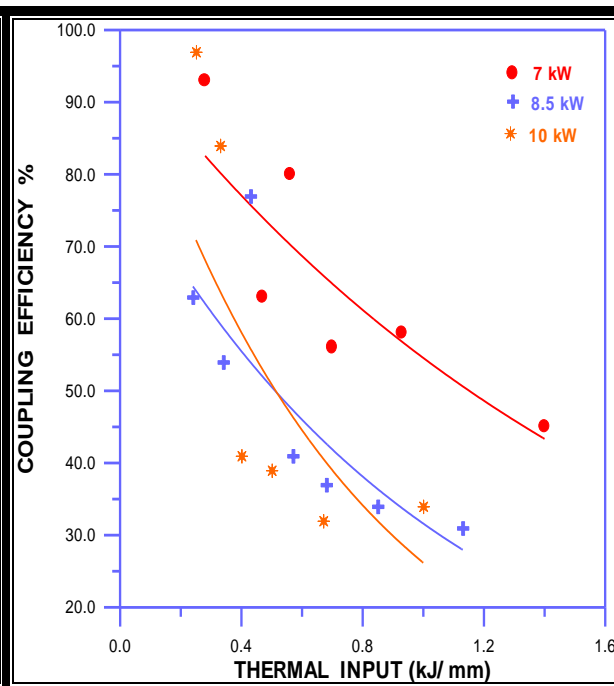


Figure (3): Thermal input versus coupling efficiency at a fixed speed and different laser power.

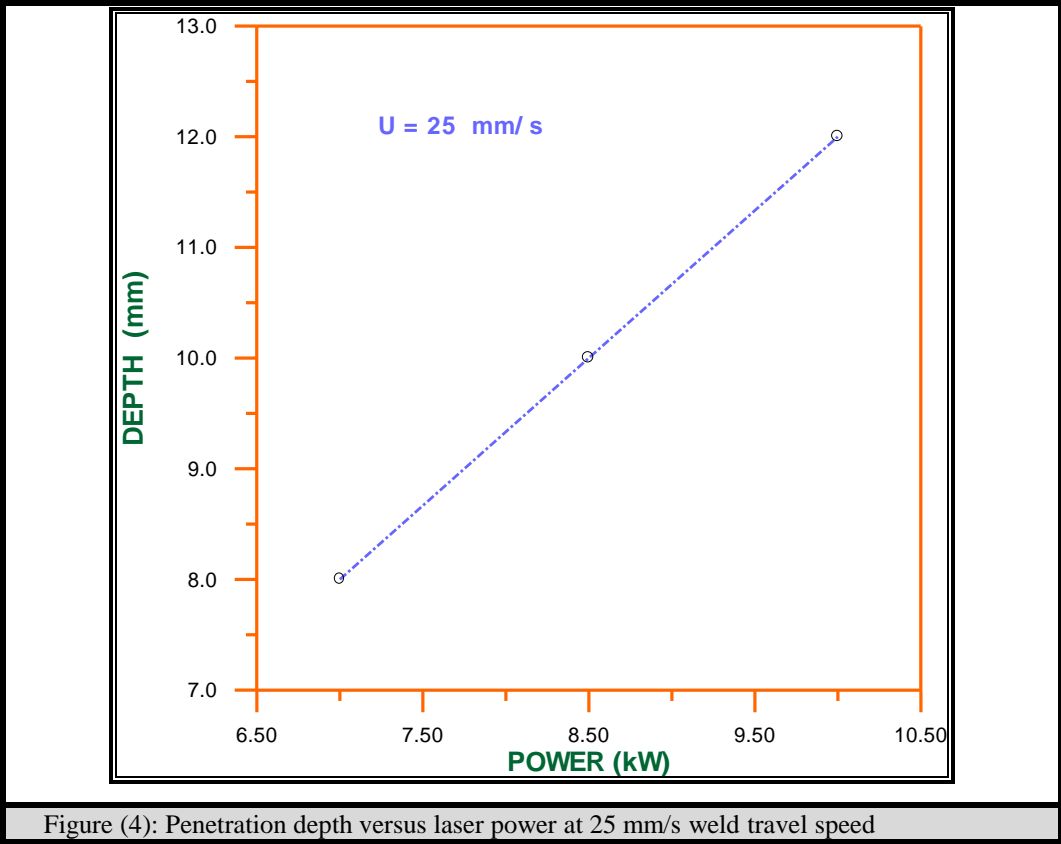
For welds 2, 14, 15 and 16, a substantial amount of the laser energy may pass out at the other end of the keyhole when it is open. We can see some jumps in the power loss for the last three samples whereas such jump is not noticeable in sample 2, may be because of the lower power and travel speed used. The line sources for the 8.5 kW welds are slightly less than those for the 7 kW welds at similar travel speeds. This could indicate a smaller spot size in these cases which are resulting from either an improved focusing or a better spatial mode structure of the beam.

The coupling efficiencies of the total powers absorbed by the mild steel when applying the 3-different laser powers are fluctuated between (45-93%) for the first power, (31-77%) for the second and (32-97%) for the third. The remaining power presumably had been lost in reflection, transmission used to ablate metal vapor or plasma from the inner

surface of the keyhole, dissipated in the vigorous fluid motion in the upper part of the weld, or lost from the bottom of the keyhole where the laser beam emerges from the for-side of the work-piece or the opening keyholes [23]. At the same time, these ratios give an indication to the limits of the power that must be used when the whole process complies with a rigid control system. Also, we can notice that the coupling efficiencies are relatively good or high for samples 4, 5, 6, 11, 13, 18 and 19. One explanation is the efficient coupling between the laser beam and the plasma in the case of CO₂ laser welding [24]. On the other hand, the decline in efficiencies for other samples could be attributed to some experimental difficulties that encountered in controlling the plume to be within an acceptable amount to benefit the absorption operation. The plume was quite weak in some welds but much stronger in others. The flaring up of the plume appears to be an essentially random event in these

welds. The penetration depth has shown explicitly a linear relationship with the range of laser power used as shown in figure (4). For higher powers, it may be expected that the relation is exponential as attributed to the high power dissipation at larger depths [21]. On the other hand, figure (5) shows the weld depth versus the travel speeds for the 3-powers used. The depth was an increasing function of the inverse of the speed. For a certain penetration depth,

if high speed is to be used, then a high power is needed. In this figure, weld depths less than 12mm indicate that thermal inputs were not enough. The 10 kW power graph is almost straight round the 12mm value indicating a full or about to be fully penetrating weld depth. To achieve a specific weld profile, the use of higher power requires a high travel speed and the opposite is true for the lower laser power levels.



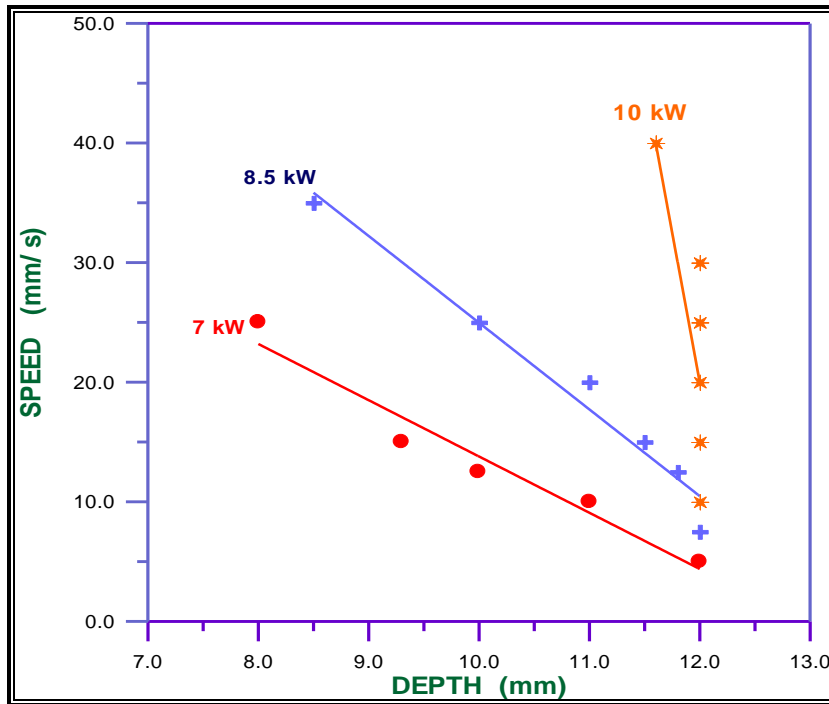


Figure (5): The speed versus penetration depth for different laser powers.

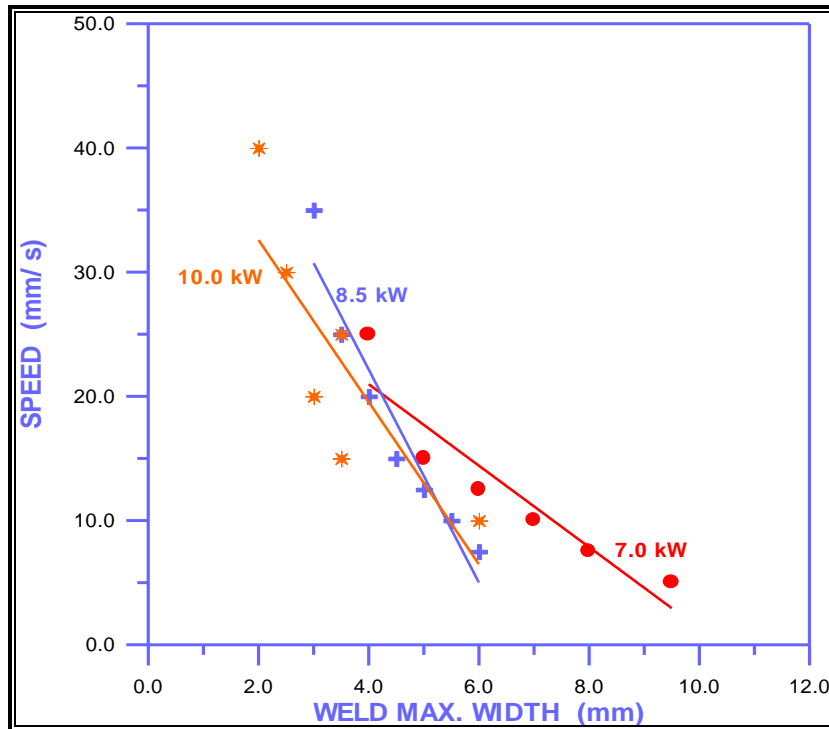


Figure (6): Weld maximum width versus speed for each power

Figure (6) shows a relation between speed and maximum weld width. In all cases, the weld width decreases as the welding speed increases

The absorbed laser power, which is the sum of point and line sources, is sketched against the coupling efficiency in figure (7). This graph shows the proportionality between the actual part of the power

that interacts with the metal and being absorbed, and the coupling efficiency. This has been taken at weld travel speed of 25 mm/s. At higher speeds, however, the coupling efficiency noticeably increased as for samples 18 and 19.

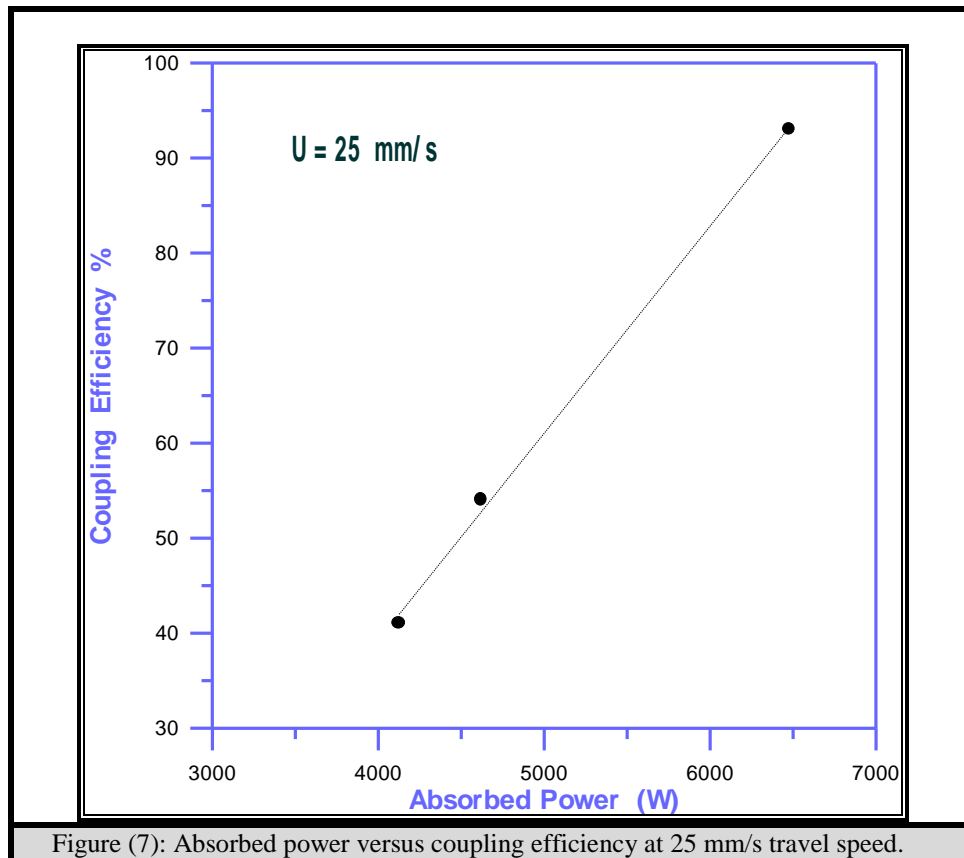


Figure (7): Absorbed power versus coupling efficiency at 25 mm/s travel speed.

The importance of a plot between welded area and thermal input emerges from its collective representation of the weld profile which can be controlled by the thermal input practically. Figure (8) illustrates this relationship where a narrow weld profile is obtained when using small thermal input while a wide profile results in from large thermal input values. It should be noticed that of up to 0.6 kJ/mm, the behavior is more or less the same for the three powers (7, 8.5 and 10 kW). At higher values of thermal input, the welded area increases more at

the lower laser power. Thermal input and welded area are more significant among other factors such as power, travel speed, top maximum width, stem width and depth to adjust the weld quality.

Figure (9) shows the experimental behavior of HAZ with the weld travel speed at different laser powers used, while Figure (10) shows a comparison between behaviors of experimental and calculated values of the HAZ lateral widths versus travel speeds for 7.0 kW input laser power. In all cases, the laser welds obtained at high travel speeds have narrower HAZ than those obtained at lower speeds.

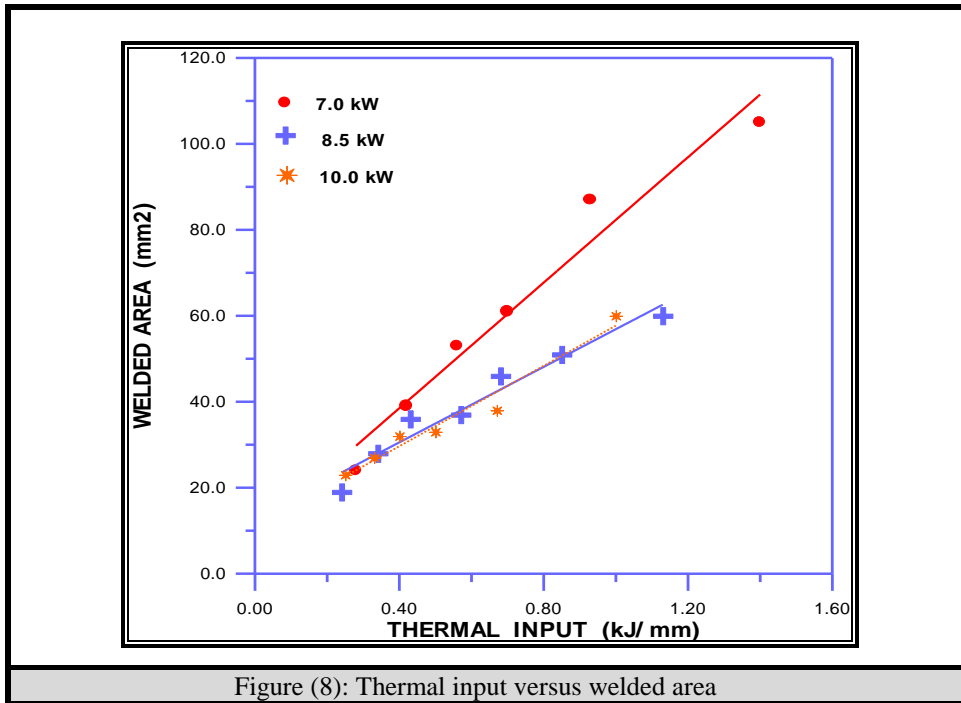


Figure (8): Thermal input versus welded area

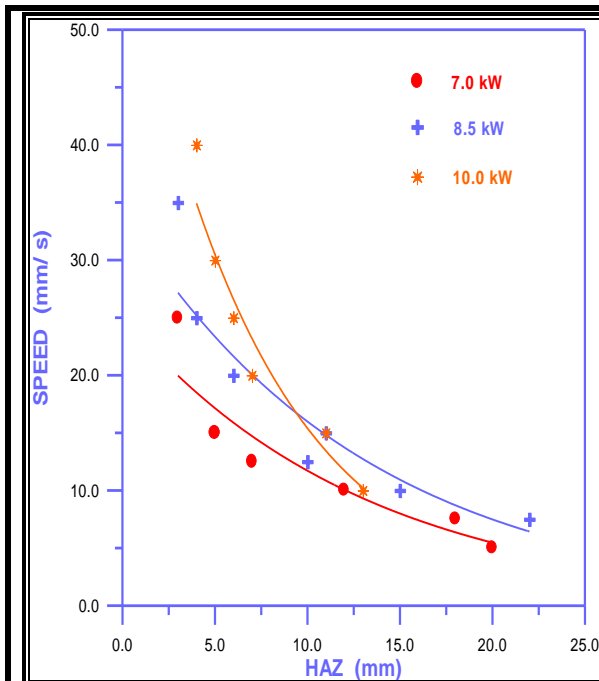


Figure (9): experimental HAZ versus speed at the different laser powers.

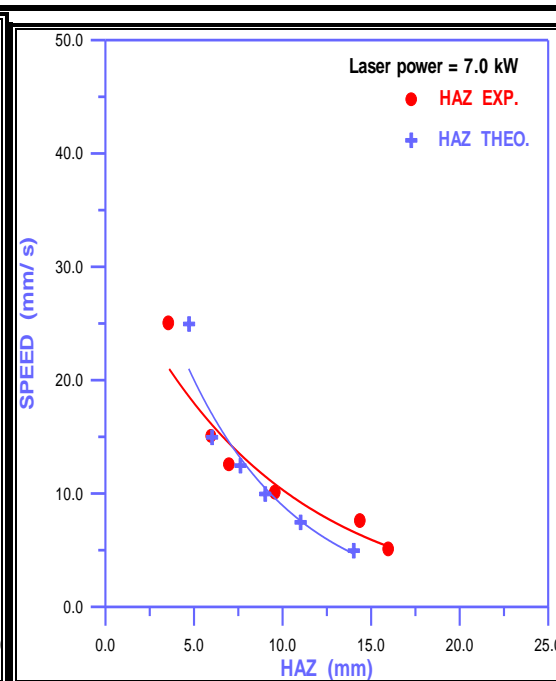
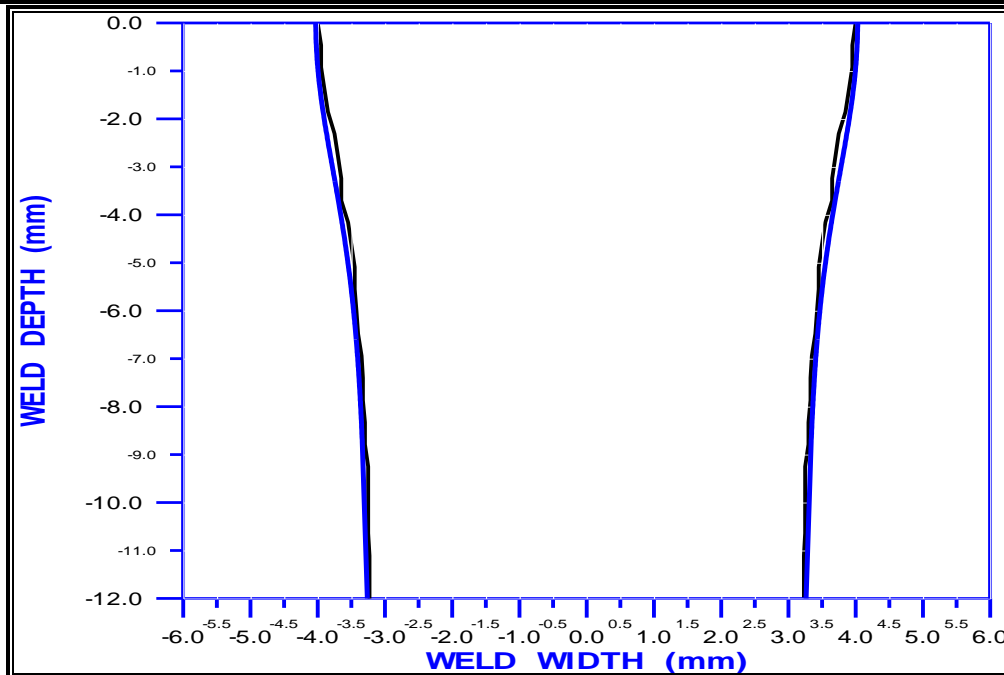


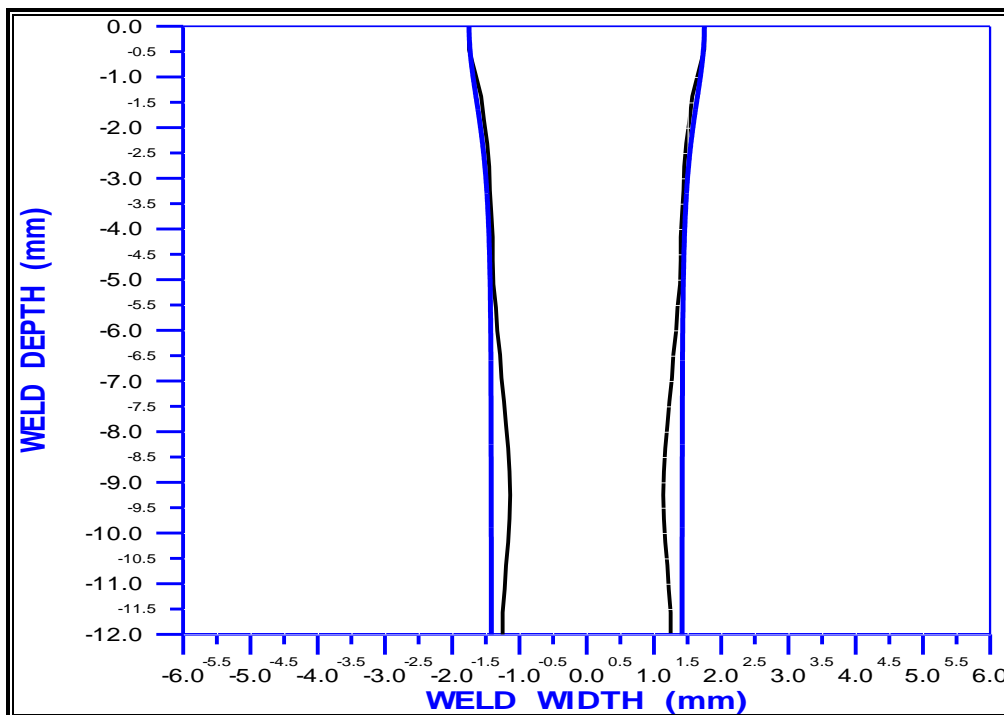
Figure (10): Experimental and Calculated HAZ against speed at 7.0kW laser.

Figure (11) shows the excellent fit between profiles of the experimental welds (solid dark) and those obtained by computation (solid light). In the partial penetration welding we considered the stem width as a radius of a circle, and then subtracted this radius value from the depth of the keyhole in order

to find the center of this circle. Using the equation of the circle we could blind the keyhole and close its terminals to approach approximately the real closing envelope, see figure (12)

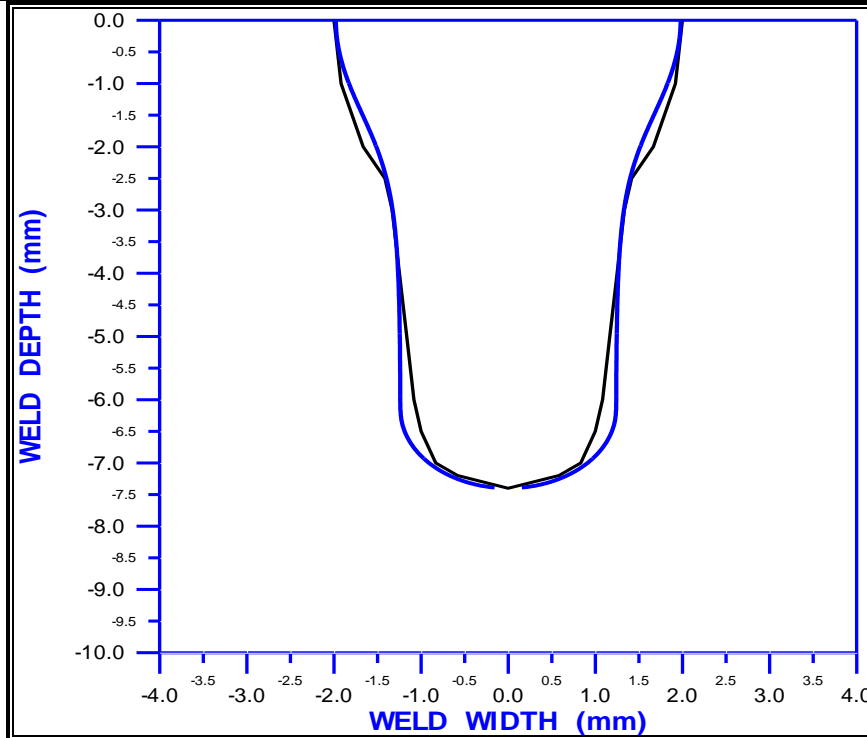


Sample -1

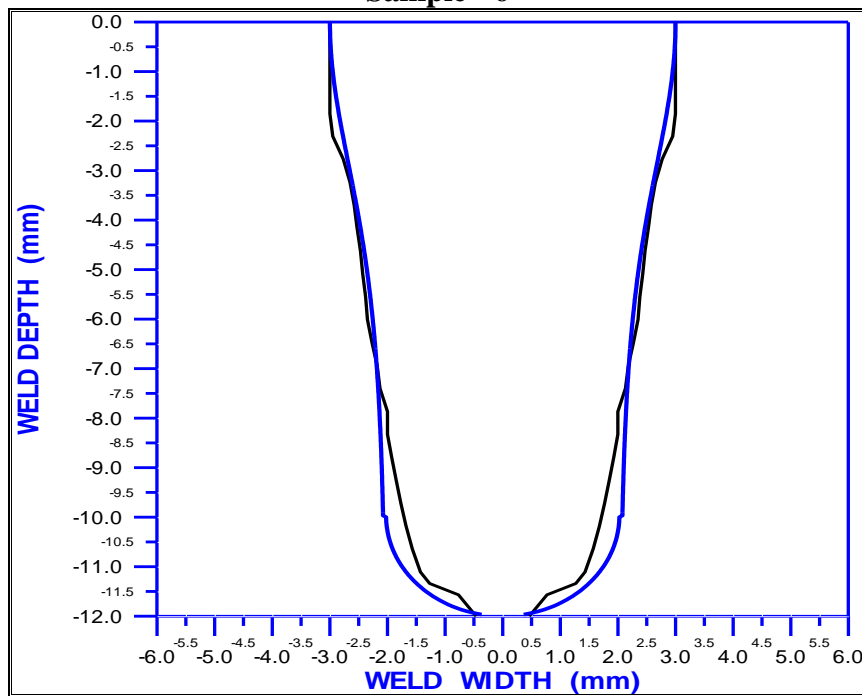


Sample -15

Figure (11): The experimental (solid dark) and calculated (solid blue) weld profiles



Sample - 6



Sample - 7

Figure (12): weld profiles of samples 6 and 7

4. Conclusion

A general modified model of deep-penetration laser welding has been constructed to provide a simple representation of a laser weld without being involved in the complicated nature of the energy interchange in the keyhole. It was possible to describe the way in which the power is absorbed through the work-piece to give interesting insights into the nature of the process. This model was used to calculate the laser power absorbed in the upper part of the weld and in the parallel-sided section. The plasma generated at high laser power increases the plume at low speeds which led to an increase in the power losses. Thermal input was inversely proportional to the coupling efficiency in contrast to the behavior of the power or speed versus the same coupling efficiency. The penetration depth has shown explicitly a linear relationship with the range of laser power used. At higher powers, the relation is exponential due to the high power dissipation at larger depths. The depth was an increasing function of the inverse of the speed. Weld depths less than 12mm indicate that thermal inputs were not enough. The 10kW power graph was almost straight around the 12mm value indicating a full penetrating weld depth. Narrow weld profile was obtained when using small thermal input values while a wide profile has resulted from large values. The unique advantage of the present model lies in its flexibility to simulate specific weld pool shapes and in its wide range of applications for different materials. It is very easy to vary laser power, travel speed, solid constants, the path of the heat source, depth as well as λ , μ and c , so that the shape of the weld pool can easily be calculated.

References

1. W. Duley, "Laser Welding" A Wiley-Inter science publication, ISBN 0-471-24679-4, (1998).
2. T. Forsman, "Laser welding of aluminum alloys", PhD Thesis, Dep. Of Materials and Manufacturing Engineering, LULEA Univ. of Technology, Dec. (2000).
3. K. Nilsson, "Technical development of the laser welding process", PhD Thesis, Department of Materials and Manufacturing Engineering, LULEA Univ. of Technology, (2001).
4. P.L. Moore, "Investigation into the microstructure and properties of laser and laser/Arc Hybrid welds in pipeline steels", PhD dissertation, Darwin College, Univ. of Cambridge, UK, Aug.11, (2003).
5. S. Chakra borty and P. Dutta, "A generalized algorithm for modeling phase change problems in materials processing", Current Science, India, 78(7), 887-891, (2000).
6. J. welingh and J. K. Kristensen, "Very deep penetration laser welding-Techniques and limitations" To be published in Pro. Of 8th NOLAMP conference, Copenhagen, Denmark, (2001).
7. Wei Han, "Computational and experimental investigations of laser drilling and welding for microelectronic packaging" PhD dissertation, Worcester Polytechnic Institute, Cambridge, 10 May, (2004).
8. J. Dowden "Dynamics of the vapor flow in the keyhole in penetration welding with a laser at medium welding process", J. Phys. D: Appl. Phys. 24, 519-532, (1991).
9. B.R. Finks, P.D. Kapadia and J. M. Dowden, " A fundamental plasma based model for energy transfer in laser material processing", J. Phys. D: Appl. Phys., 23 , 643-654, (1990).
10. A. Kar and J. Mazumder, "Mathematical modeling of a keyhole laser welding", J. Appl. Phys. 78(11), 6353-6360, (1995).
11. R. Ducharm Jon A. Sales, A. J. Richmanl, "The laser welding of thin metal sheets: an integrated keyhole and weld pool model with supporting experiments", J. Phys. D: Appl. Phys., 27, 1619-1627, (1994).
12. K.Y. Benyouni^s, A.G. Olabiand M.S.J. Hashmi, "Multi-response optimization of CO₂ laser-welding process of austenitic stainless, Optics & Laser Technology, 40(1), 76-87 (2008).
13. Guohua Li , Yan Cai and Yixiong Wu, "Stability information in plasma image of high-power CO₂ laser welding" Optics and Lasers in Engineering, Volume 47, Issue 9, pp. 990-994 (2009) .
14. Hongxiao Wang, Chunsheng Wang, Chunyuan Shi, Guangzhong He, Ting Wang, and Jingfei Xiao "The study of laser welding parameters influence on fusion zone shape and surface quality of SUS301L stainless steel" International Journal of Applied Engineering Research (report), USA, (2009).
15. Y. Kawahito, M. Mizutani, S. Katayama "High quality welding of stainless steel with 10 kW high power fiber laser" Science and Technology of Welding & Joining, Volume 14, Number 4, pp. 288-294(7) (2009).

16. Chengyun Cui, Jiandong Hu, Kun Gao, Shulai Pang, YueYang, Hongying Wang and Zuoxing Guo, "Effects of Process Parameters on Weld Metal Keyhole Characteristics with CO₂ Laser Butt Welding" *Lasers in Eng.*, Vol. 18, pp. 319–327, (2008).
17. Hong Wang, Yaowu Shi and Shuili Gong, "Numerical simulation of laser keyhole welding processes based on control volume methods, Journal of Physics D: Applied Physics Create an alert RSS this journal J. Phys. D: Appl. Phys. 39 4722, Volume 39, Number 21 (2006) doi: 10.1088/0022-3727/39/21/032.
18. K.I. Hyungson, P.S. Mohanty and J. Mazumder, "Modeling of laser keyhole welding: Part1, Mathematical modeling, Numerical Methodology", *Metallurgical & Materials Transactions A*, 33A, 1817-1831, (2002).
19. J. Klastrup Kristeen et al, "Laser welding of aluminum alloys-process and properties", Proc. Of 8th NOLAMP conference, Denmark, (2001).
20. E.A. Metzbower, "Laser beam welding: Thermal Profiles and HAZ hardness ", *Welding J.*, 69(7), 272-s to 278-s, (1990).
21. Walid K. Hamoudi, Adel K. Hamoudi and Saad A. M. Salih, "Modeling of 3-D Keyhole Co₂ Laser welding of Steel" *IJAP*, 6(1), 15-21 (2010).
22. Adel K. Hamoudi, Walid K. Hamoudi and Saad A. M. Salih, "HAZ and temperature distribution of CO₂ laser 3-D laser welding, accepted for publication NSMT (2010)
23. . Dowden, P. Kapadia and N. Postacioglu, "An analysis of laser keyhole welding", *J. Phys. D: Appl. Phys.*, 22 , 741-749, (1989).
24. R.V. Arutyunyan, V.Y. Baranov and V.Y. Bolshov, "Thermo-hydrodynamic models of the interaction of pulsed-periodic radiation with matter", *SOV.J. Quant. Elect.*, 17(2), 163-168, (1987).